JAM CM Journal of Applied Mathematics and Computational Mechanics 2024, 23(4), 76-88
www.amcm.pcz.pl p-ISSN 2299-9965
DOI: 10.17512/jamcm.2024.4.07 e-ISSN 2353-0588

SYNCHRONIZATION FOR A CLASS OF PROPORTIONAL CAPUTO FRACTIONAL-ORDER NEURAL NETWORKS

Abdelhameed Mohamed Nagy[1,2], *Abdellatif Ben Makhlouf*[3], *Abdulaziz Alsenafi*[1]
Fares Alazemi[1]

[1] *Department of Mathematics, College of Science, Kuwait University, Safat, Kuwait*
[2] *Department of Mathematics, Faculty of Science, Benha University, Benha, Egypt*
[3] *Department of Mathematics, Faculty of Sciences of Sfax, University of Sfax, Sfax, Tunisia*
abdelhameed_nagy@yahoo.com, abdulaziz.alsenafi@ku.edu.kw, fares.alazemi@ku.edu.kw
abdellatif.benmakhlouf@fss.usf.tn

Received: 30 June 2024; Accepted: 27 October 2024

Abstract. Synchronization of fractional order systems has gained great interest in various research activities in recent years. The aim of this study is to investigate the synchronization of a class of neural network systems with respect to the proportional Caputo fractional order derivative. Using the generalized Gronwall inequality, a sufficient condition that possesses the exponential convergence rate, presents and demonstrates that the error of the proposed system converges to zero. Two illustrative numerical examples are provided to show the applicability and validity of the obtained theoretical results.

MSC 2010: *26A33, 39B82, 60H10*
Keywords: *synchronization, generalized Gronwall inequality, neural networks*

1. Introduction

Fractional calculus has shown to be a significant tool in modeling numerous phenomena in the domains of engineering, physics, and economics [1-5]. The crucial distinction between fractional order derivatives (FODs) and their integer counterparts is that FODs have a non-local property. In evaluating the fractional order derivatives (FODs) of a provided function, non-local FOD operators require the complete history of the function. The non-local characteristic of FODs makes them more accurate and appropriate than integer order derivatives [6]. As a result, many researchers utilize FODs to characterize a wide range of real-world processes in chemical biology, physical science, mathematical biology, viscoelasticity, and electro-chemistry. The Riemann-Liouville and Caputo models are the most researched and used definitions of fractional derivatives. In recent years, several formulations of fractional calculus have emerged in literature, such as the Atangana-Baleanu derivative, Caputo--Fabrizio derivative, and the one we are interested in, the proportional Caputo fractional (PCF) derivative. For more details, see [7-18] and the references therein.

Neural networks have received a lot of attention in a variety of fields. Meanwhile, numerous researchers have extended and applied the neural networks for the fractional-order case in order to create fractional neural models. It is also worth noting that fractional-order neural networks (FONNs) have been shown to be quite effective in many applications, and some outstanding results have been obtained when studying them (see [19-21]).

Recently, the synchronization of fractional-order systems in secure communication and control processing has garnered significant attention. Furthermore, the field of synchronization of neural networks has attracted a lot of interest due to its various applications, such as parallel image processing, biological systems, secure communication, and so on [20, 22]. Additionally, there are also some recent publications that investigate chaotic synchronization in FONNs [23, 24]. Numerous researchers have examined the synchronization of fractional-order systems with varying definitions of the fractional derivatives. However, as far as we know, there is a dearth of research on the synchronization of fractional derivatives with respect to the proportional Caputo fractional order. Based on this, the major goal of this article is to investigate the synchronization neural network in terms of the proportional Caputo derivative.

The remaining sections of the paper are arranged as follows. Section 2 presents certain calculus definitions that are relevant to our current study. The main results of this investigation are provided in Section 3. Section 4 contains numerical experiments that are used to validate the main proposed results. Conclusions are provided in Section 5.

2. Preliminaries

Definition 1 (see [16]) the PCF integral of f of order $\mu, \mu > 0$, and $\eta \in (0,1]$ is defined by

$$\mathscr{I}_a^{\mu,\eta} f(\nu) = \frac{1}{\eta^{\mu}\Gamma(\mu)} \int_a^{\nu} e^{\frac{\eta-1}{\eta}(\nu-\kappa)} (\nu-\kappa)^{\mu-1} f(\kappa)\, \mathrm{d}\kappa.$$

Definition 2 (see [16]) the PCF derivative of f of order $\mu, \mu \in (0,1)$, and $\eta \in (0,1]$ is defined by

$$\begin{aligned} \mathscr{D}_a^{\mu,\eta} f(\nu) &= \left(\mathscr{D}^{\eta}\ \mathscr{I}_a^{1-\mu,\eta} f\right)(\nu) \\ &= \frac{\mathscr{D}^{\eta}}{\eta^{1-\mu}\Gamma(1-\mu)} \int_a^{\nu} e^{\frac{\eta-1}{\eta}(\nu-\kappa)} (\nu-\kappa)^{-\mu} f(\kappa)\, \mathrm{d}\kappa, \end{aligned} \tag{1}$$

where

$$\mathscr{D}^{\eta} f(\nu) = (1-\eta) f(\nu) + \eta f'(\nu).$$

Definition 3 (see [16]) the PCF derivative of f with $\mu \in (0,1)$ and $\eta \in (0,1]$ is defined by

$$^{\mathrm{C}}\mathscr{D}_a^{\mu,\eta} f(\nu) = \mathscr{D}_a^{\mu,\eta}\left(f(\nu) - f(a)e^{\frac{\eta-1}{\eta}(\nu-a)}\right).$$

Lemma 1 (see [25]) For $\mu \in (0,2]$, we have

$$E_{\mu,1}(\lambda^{\mu}) \sim \frac{\exp(\lambda)}{\mu}, \ \ \lambda \longmapsto \infty.$$

3. Main results

Consider the following proportional fractional-order neural networks

$$^{\mathrm{C}}\mathscr{D}_0^{\mu,\eta}\xi(\nu) = -a_i\xi(\nu) + \sum_{j=1}^{n} b_{ij} f_j\big(\xi(\nu)\big) + J_i, \quad i = 1,2,...,n. \tag{2}$$

Equation (2) can be recast in a matrix form as follows:

$$^{\mathrm{C}}\mathscr{D}_0^{\mu,\eta}\xi(\nu) = -A\xi(\nu) + Bf\big(\xi(\nu)\big) + J, \quad \nu \geq 0, \tag{3}$$

where $A = diag(a_i)$, $a_i > 0$, $i = 1,2,\ldots,n$. The number n denotes the number of neurons in the network. The vector $f\big(\xi(\nu)\big) = [f_1\big(\xi(\nu_1)\big), f_2\big(\xi(\nu_2)\big), \ldots, f_n\big(\xi(\nu_n)\big)]^T$ is the neuron activation function; $\xi(\nu) = [\xi_1(\nu), \xi_2(\nu), \ldots, \xi_n(\nu)]^T \in \mathbb{R}^n$; $B = \{b_{ij}\} \in \mathbb{R}^{n\times n}$ represents the connection between the i-th and j-th neurons; $J = [J_1, J_2, \ldots, J_n]^T$ is an external input vector.

Set the following assumption:
$\mathscr{H}_1$: f_i satisfies

$$|f_i(\chi_1) - f_i(\chi_2)| \leq L_i|\chi_1 - \chi_2|, \tag{4}$$

where $L_i > 0$.

Remark 1 Let $L = \max\limits_{1\leq i\leq n}(L_i)$. Then

$$||f(\chi_1) - f(\chi_2)|| \leq L||\chi_1 - \chi_2||. \tag{5}$$

3.1. Synchronization

This subsection addresses the synchronization of proportional fractional-order neural networks using linear control. Let us assume that system (3) is the drive system, and the response system is given as follows:

$$^{\mathrm{C}}\mathscr{D}_0^{\mu,\eta}\zeta_i(\nu) = -a_i\zeta_i(\nu) + \sum_{j=1}^{n} b_{ij} f_j\big(\zeta_j(\nu)\big) + J_i + \mathscr{C}_i(\nu), \quad i = 1,2,...,n. \tag{6}$$

or

$$^{\mathrm{C}}\mathscr{D}_0^{\mu,\eta}\zeta(\nu) = -A\zeta(\nu) + Bf\big(\zeta(\nu)\big) + J + \mathscr{C}(\nu), \quad \nu \geq 0, \tag{7}$$

where $\mathscr{C}(\nu) \in \mathbb{R}^n$ is a controller that will be provided subsequently.
If we consider the error vector $\mathscr{E}(\nu) = \zeta(\nu) - \xi(\nu)$, then

$$^{\mathrm{C}}\mathscr{D}_0^{\mu,\eta}\mathscr{E}(\nu) = -A\mathscr{E}(\nu) + Bg\big(\mathscr{E}(\nu)\big) + \mathscr{C}(\nu), \quad \nu \geq 0, \tag{8}$$

where $g\big(\mathscr{E}(\nu)\big) = f\big(\zeta(\nu)\big) - f\big(\xi(\nu)\big)$.
To identify synchronization, we assume that the fractional-order neural network is synced by a controller chosen as follows:

$$\mathscr{C}(\nu) = -Q\mathscr{E}(\nu),$$

where $Q = diag(q_1, q_2, \ldots, q_n)$, $q_i > 0$, is called the gain matrix.
Therefore, the synchronization error system (8) can be written as follows:

$$^{\mathrm{C}}\mathscr{D}_0^{\mu,\eta}\mathscr{E}(\nu) = -\tilde{C}\mathscr{E}(\nu) + Bg\big(\mathscr{E}(\nu)\big), \quad \nu \geq 0, \tag{9}$$

where $\tilde{C} = A + Q$.
In what follows, we demonstrate that the solution of the synchronization error system (8) converges to zero, which confirms that synchronization occurs.

Theorem 1 Assume that assumption $\mathscr{H}_1$ is satisfied. Then, the solution of the system (9) converges to zero, if the following condition holds:

$$\lambda = \frac{1 - \Big(\eta + \Gamma(\mu)^{\frac{1}{\mu}} L^{\frac{1}{\mu}} k^{\frac{1}{\mu}} \|B\|^{\frac{1}{\mu}}\Big)}{\eta} > 0,$$

where

$$k = \sup_{r \geq 0} ||E_{\mu,\mu}(-\tilde{C}r^{\mu})||.$$

PROOF The solution of the system (9) is provided by

$$\begin{aligned}\mathscr{E}(\nu) = {} & E_{\mu,1}(-\tilde{C}\frac{\nu^{\mu}}{\eta^{\mu}})e^{\frac{(\eta-1)}{\eta}\nu}\mathscr{E}(0) + \\ & \eta^{-\mu}\int_0^{\nu} e^{\frac{(\eta-1)}{\eta}(\nu-s)}(\nu-s)^{\mu-1}E_{\mu,\mu}\big(-\tilde{C}(\frac{\nu-s}{\eta})^{\mu}\big)B[f\big(\zeta(s)\big) - f\big(\xi(s)\big)]ds.\end{aligned} \tag{10}$$

Therefore

$$\begin{aligned}||\mathscr{E}(\nu)|| \leq {} & e^{\frac{(\eta-1)}{\eta}\nu}||\mathscr{E}(0)|| + \\ & \eta^{-\mu}L\int_0^{\nu} e^{\frac{(\eta-1)}{\eta}(\nu-s)}(\nu-s)^{\mu-1}||E_{\mu,\mu}\big(-\tilde{C}(\frac{\nu-s}{\eta})^{\mu}\big)||\,\|B\|\,\|\mathscr{E}(s)\|ds\end{aligned} \tag{11}$$

Let $G(\nu) = e^{\frac{(1-\eta)}{\eta}\nu}||\mathscr{E}(\nu)||$. Thus

$$G(\nu) \leq ||\mathscr{E}(0)|| + kL\eta^{-\mu}\|B\| \int_0^\nu (\nu - s)^{\mu-1} G(s)ds. \tag{12}$$

Using generalized Gronwall inequality (see [26]), we get

$$G(\nu) \leq ||\mathscr{E}(0)||E_{\mu,1}\big(\Gamma(\mu)\frac{Lk\|B\|}{\eta^\mu}\nu^\mu\big). \tag{13}$$

According to Lemma 1, there exists $M > 0$ such that

$$\begin{aligned} ||\mathscr{E}(\nu)|| &\leq e^{\frac{(\eta-1)}{\eta}\nu}E_{\mu,1}\big(\Gamma(\mu)\frac{Lk\|B\|}{\eta^\mu}\nu^\mu\big)||\mathscr{E}(0)|| \\ &\leq Me^{\frac{(\eta-1)}{\eta}\nu}e^{\left(\frac{\Gamma(\mu)Lk\|B\|}{\eta^\mu}\right)^{\frac{1}{\mu}}\nu}||\mathscr{E}(0)|| \\ &\leq Me^{-\lambda\nu}||\mathscr{E}(0)||. \end{aligned} \tag{14}$$

■

4. Numerical experiments

In this section, two illustrative numerical examples will be provided to demonstrate and verify the theoretical results given in Section 2. The numerical technique used to solve the proposed problem relies on a decomposition formula for the proportional Caputo derivative, which is described in Ref. [13].

Example 1 Consider the following three-dimensional FONN as follows:

$$\begin{cases} \mathscr{D}_0^{\mu,\eta}\xi_1 = -\xi_1 + 0.03\tanh\xi_1 - 0.09\tanh\xi_2 + 0.5, \\ \mathscr{D}_0^{\mu,\eta}\xi_2 = -\xi_2 + 0.06\tanh\xi_1 + 0.09\tanh\xi_2 + 0.06\tanh\xi_3 + 1, \\ \mathscr{D}_0^{\mu,\eta}\xi_3 = -\xi_2 - 0.03\tanh\xi_1 + 0.09\tanh\xi_3 + 1.5, \end{cases} \tag{15}$$

where $\mu = 0.95$, $\eta = 0.8$, $\xi(\nu) = [\xi_1(\nu)\ \xi_2(\nu)\ \xi_3(\nu)]^T$, $A = diag(1,1,1)$, $J = [0.5\ 1\ 1.5]^T$, $f(\xi(\nu)) = 0.03[\tanh(\xi_1(\nu))\ \tanh(\xi_2(\nu))\ \tanh(\xi_3(\nu))]^T$ and

$$B = \begin{bmatrix} 1 & -3 & 0 \\ 2 & 3 & 2 \\ -1 & 0 & 3 \end{bmatrix}.$$

In the response system, we pick out the elements of the gain feedback as $q_1 = 4$, $q_2 = 3$, and $q_3 = 4$. We can observe from the data that the nonlinear function $\tanh(\cdot)$ satisfies the Lipschitz condition with the Lipschitz constant $L = 0.03$. Moreover, we have $\|B\| = 7$ and $k = \sup_{\nu\geq 0}\|E_{\mu,\mu}(-\tilde{C}\nu^\mu)\| \approx 1$.

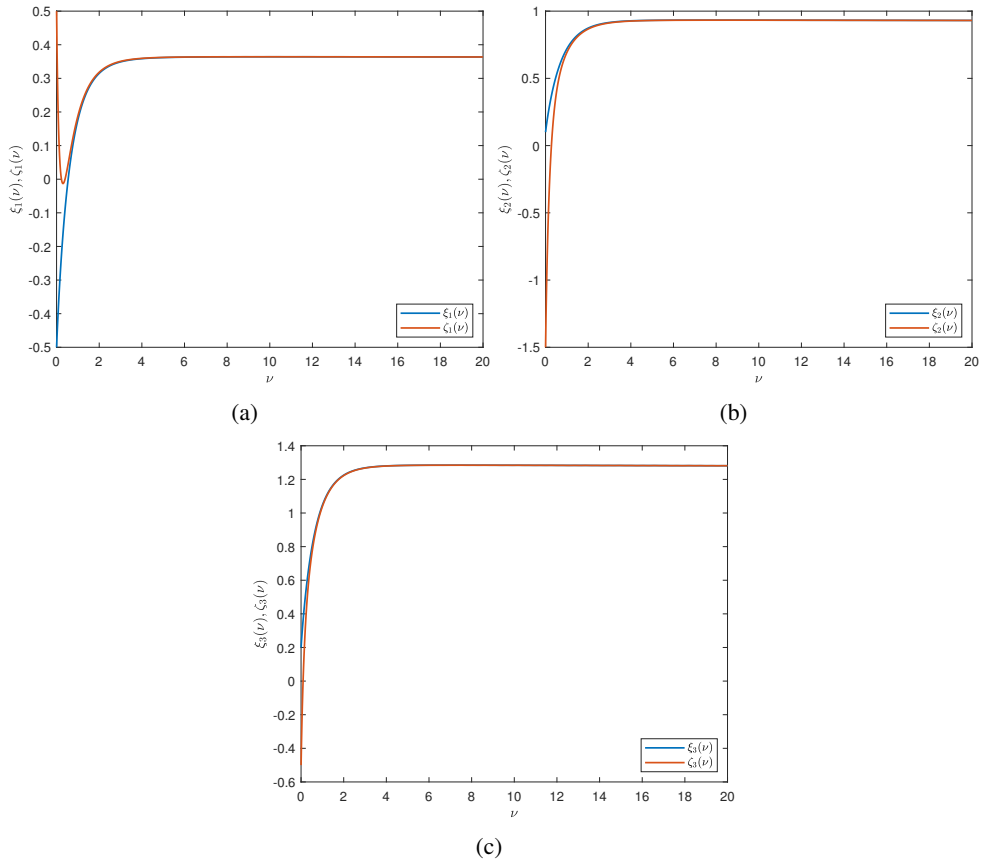

Fig. 1. Trajectories of the drive and response systems of Example 1 with $\mu = 0.95$, and $\eta = 0.8$

This implies that $\lambda = \dfrac{1-[\eta+(\Gamma(\mu)\|B\|Lk)^{\frac{1}{\mu}}]}{\eta} = 0.0086 > 0$. Thus, the conditions of Theorem 1 are satisfied, and we can accomplish the synchronization between drive and response systems. The trajectories of the drive and response systems are depicted in Figure 1. Furthermore, Figure 2 depicts the synchronization error. Additionally, the effects of parameters μ and η on the synchronization error of the drive and response systems at $\mu = 0.99$, $\eta = 0.95$ and $\mu = \eta = 0.75$, respectively, as well as the time response of two systems are displayed in Figures 3-6. According to the numerical results, the aforementioned systems are exponentially synchronized, which validates the theoretical results.

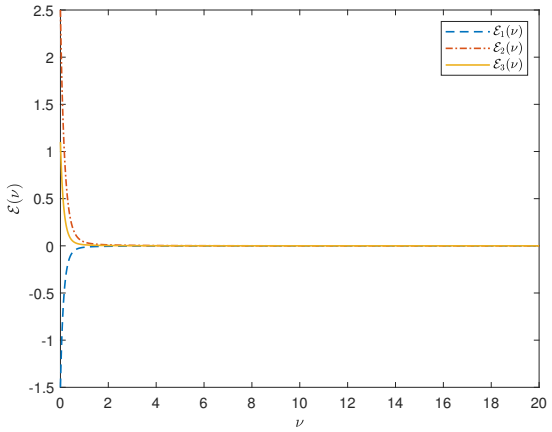

Fig. 2. The trajectories of synchronization error for Example 1 at $\mu = 0.95$, and $\eta = 0.8$

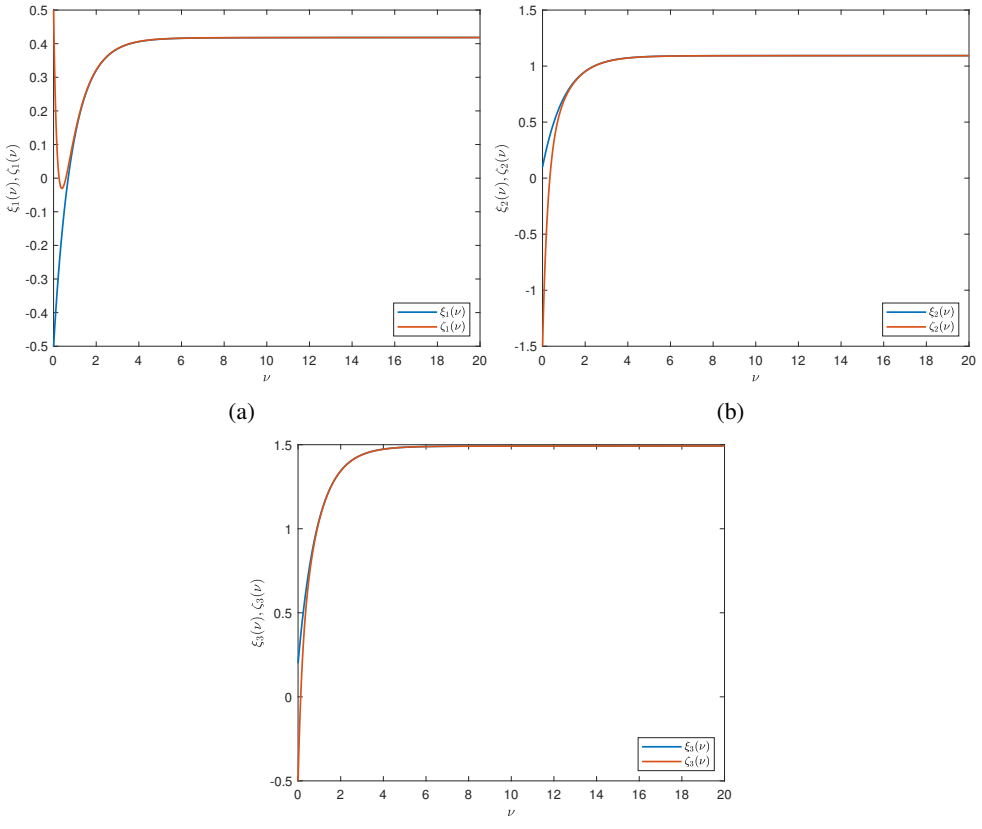

Fig. 3. Trajectories of the drive and response systems of Example 1 with $\mu = 0.99$, and $\eta = 0.95$

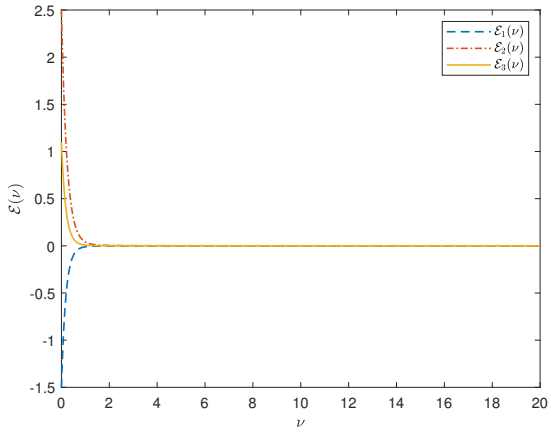

Fig. 4. The trajectories of synchronization error for Example 1 at $\mu = 0.99$, and $\eta = 0.95$

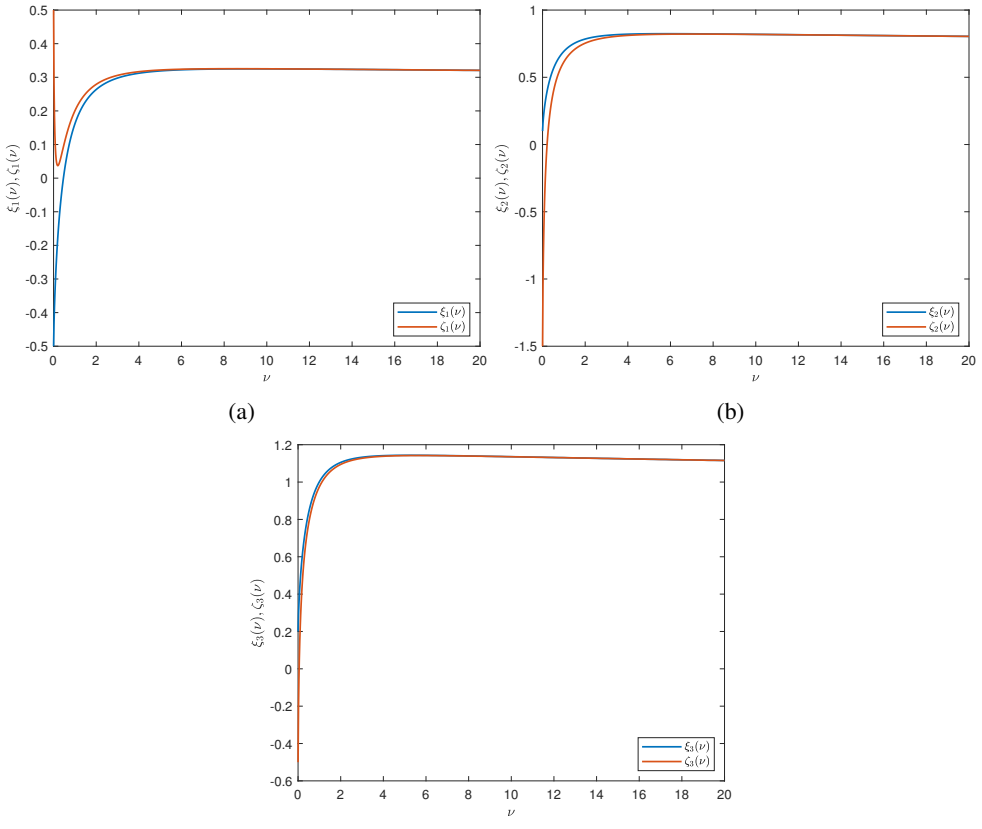

Fig. 5. Trajectories of the drive and response systems of Example 1 with $\mu = 0.75$, and $\eta = 0.75$

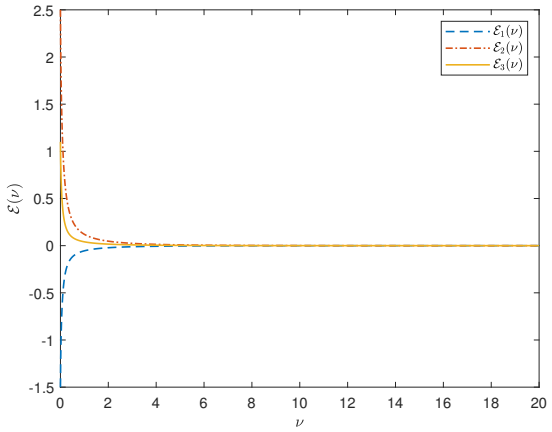

Fig. 6. The trajectories of synchronization error for Example 1 at $\mu = 0.75$, and $\eta = 0.75$

Example 2 Consider the FONN system given in (2) with $\mu = 0.9$, $\eta = 0.75$, $\xi(\nu) = [\xi_1(\nu) \;\; \xi_2(\nu) \;\; \xi_3(\nu)]^T$, $A = diag(1,1,1)$, $J = [1 \;\; 1.5 \;\; 2.5]^T$, $f(\xi(\nu)) = 0.01[\sin(\xi_1) \; \sin(\xi_2) \; \sin(\xi_3)]^T$ and

$$B = \begin{bmatrix} 2 & -1 & -3 \\ -3 & 2 & 1 \\ 1 & -3 & 2 \end{bmatrix}.$$

In the response system, we select the coefficients of the gain feedback as $q_1 = 1$, $q_2 = 2$ and $q_3 = 3$. It is obvious that the nonlinear function $\sin(\cdot)$ satisfies the Lipschitz criterion with $L = 0.01$. In addition, we have $\|B\| = 6$ and $k = \sup_{\nu \geq 0} \|E_{\mu,\mu}(-C\nu^{\mu})\| \approx 1$. Accordingly, $\lambda = \dfrac{1 - [\eta + (\Gamma(\mu)\|B\|Lk)^{\frac{1}{\mu}}]}{\eta} =$ $= 0.2750 > 0$. As a result, the prerequisites of Theorem 1 are met, and therefore synchronization occurs between the drive and response systems. Figures 7 and 8 demonstrate the trajectories of the systems $\xi(\nu)$ and $\zeta(\nu)$, as well as the synchronization error. Moreover, Figures 9 and 10 show the trajectories of the systems $\xi(\nu)$ and $\zeta(\nu)$, and their synchronization error at $\mu = 0.7$, and $\eta = 0.75$, respectively. It is evident from numerical simulations that the FONNs are synchronized and attained after a short transient period. This aligns flawlessly with the obtained theoretical outcomes.

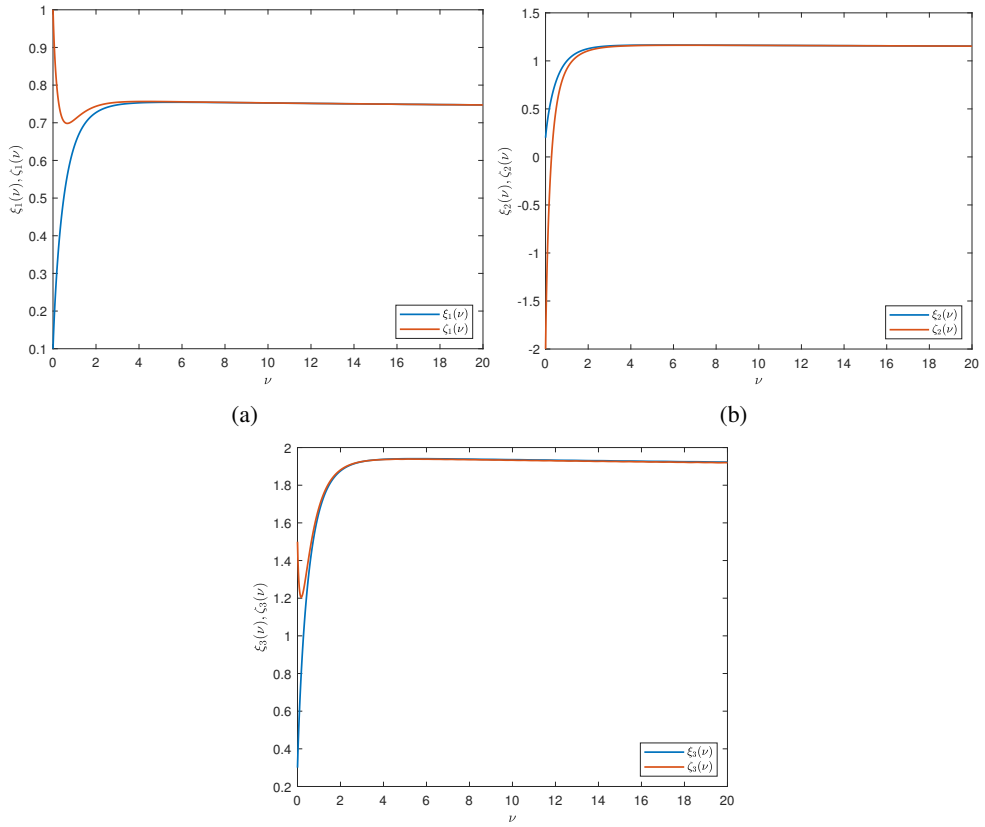

Fig. 7. Trajectories of the drive and response systems of Example 2 with $\mu = 0.9$, and $\eta = 0.75$

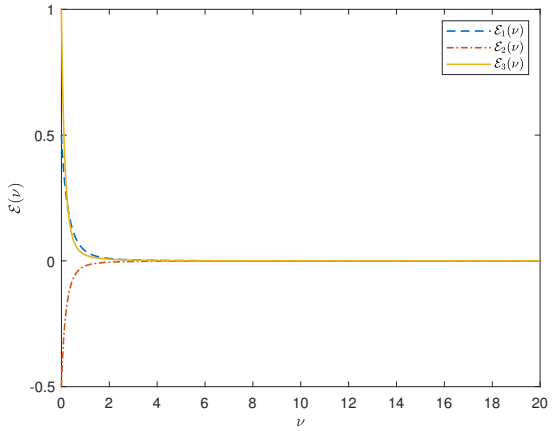

Fig. 8. The trajectories of synchronization error for Example 2 at $\mu = 0.9$, and $\eta = 0.75$

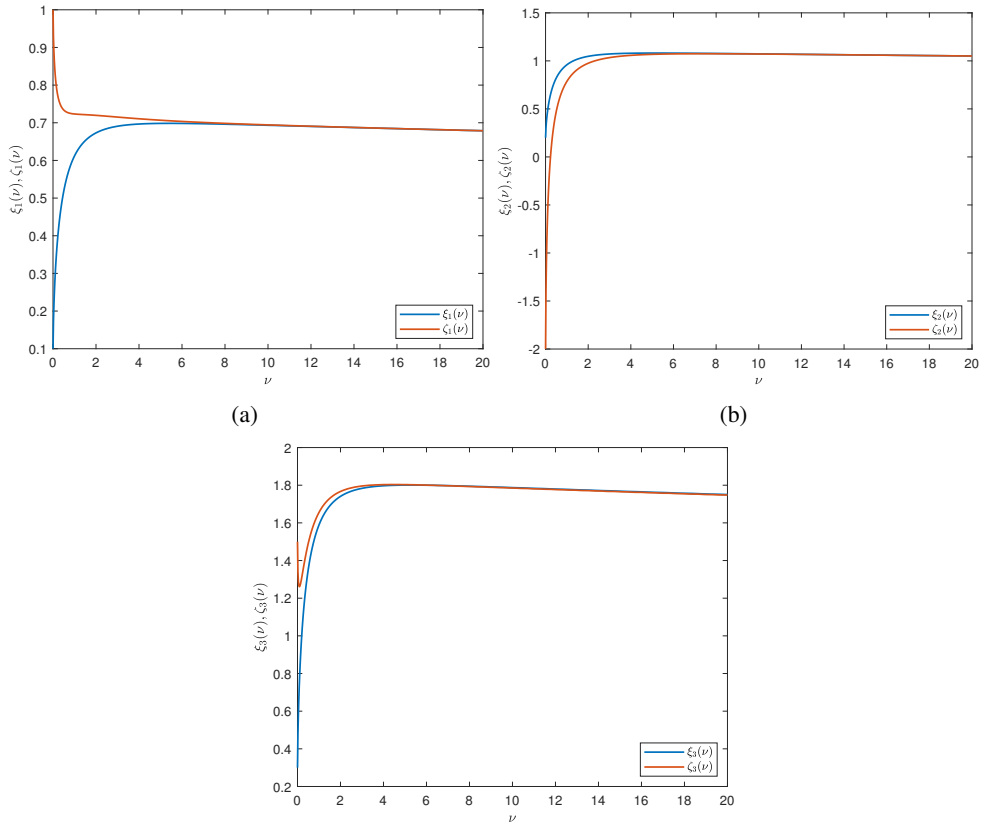

Fig. 9. Trajectories of the drive and response systems of Example 2 with $\mu = 0.7$, and $\eta = 0.75$

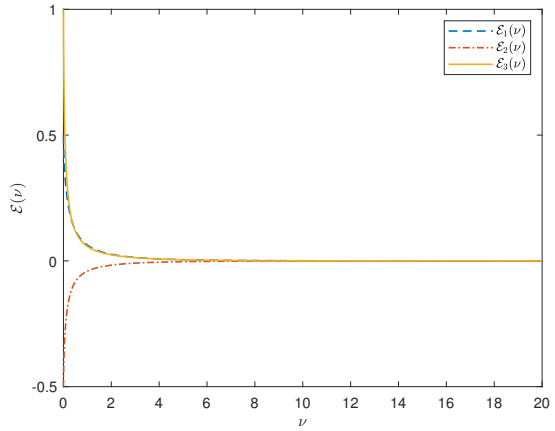

Fig. 10. The trajectories of synchronization error for Example 2 at $\mu = 0.7$, and $\eta = 0.75$

5. Conclusion

Synchronization of fractional order systems has garnered significant attention recently due to its potential applications in control processing and secure communication. Synchronization of fractional-order systems has been examined by several authors. However, as far as we know, the results on synchronization of a class of proportional Caputo FONNs are limited. Based on that, the main goal is this paper to investigate the neural network synchronization in the sense of the proportional Caputo fractional derivative. Using the Gronwall inequality, it is demonstrated that the synchronization error converges to zero. Additionally, to validate and verify the given theoretical analysis, two numerical experiments are provided. The simulation results showed that they coincide with the theoretical analysis. Finally, it is worth mentioning that the proposed idea can be prospectively extended for other types of fractional definitions.

Funding

This work was supported and funded by Kuwait University, research grant no. SM04/20.

References

[1] Kilbas, A.A., Srivastava, H.M., & Trujillo, J.J. (2006). *Theory and Applications of Fractional Differential Equations*. Amsterdam: Elsevier.

[2] Koeller, R. (1984). Applications of fractional calculus to the theory of viscoelasticity. *ASME Journal of Applied Mechanics*, *51*, 299-307.

[3] Lazarević, M.P. (2006). Finite time stability analysis of PD^{α} fractional control of robotic time-delay systems. *Mechanics Research Communications*, *33*(2), 269-279.

[4] Nagy, A.M. (2022). Numerical solutions for nonlinear multi-term fractional differential equations via Dickson operational matrix. *International Journal of Computer Mathematics*, *99*(7), 1505-1515.

[5] Nagy, A.M., Assidi, S., & Makhlouf, A.B. (2022). Convergence of solutions for perturbed and unperturbed cobweb models with generalized Caputo derivative. *Boundary Value Problem*, *2022*, 89.

[6] Lynch, V.E., Carreras, B.A., del-Castillo-Negrete, D., Ferreira-Mejias, K.M., & Hicks, H.R. (2003). Numerical methods for the solution of partial differential equations of fractional order. *Journal of Computational Physics*, *192*(2), 406-421.

[7] Baleanu D., Jajarmi, A., Mohammadi, H., & Rezapour, S. (2020). A new study on the mathematical modelling of human liver with Caputo-Fabrizio fractional derivative. *Chaos, Solitons & Fractals*, *134*, 109705.

[8] Mohammadi, H., Kumar, S., Rezapour, S., & Etemad, S. (2021). A theoretical study of the Caputo-Fabrizio fractional modeling for hearing loss due to Mumps virus with optimal control. *Chaos, Solitons & Fractals*, *144*, 110668.

[9] Khan, H., Alam, K., Gulzar, H., Etemad, S., & Rezapour, S. (2022). A case study of fractal--fractional tuberculosis model in China: Existence and stability theories along with numerical simulations. *Mathematics and Computers in Simulation*, *198*, 455-473.

[10] Yadav, P., Jahan, S., & Nisar, K.S. (2023). Fractional order mathematical model of Ebola virus under Atangana-Baleanu-Caputo operator. *Results in Control and Optimization*, *13*, 100332.

[11] Wali, M., Arshad, S., Eldin, S.M., & Siddique, I. (2023). Numerical approximation of Atangana--Baleanu Caputo derivative for space-time fractional diffusion equations. *AIMS Mathematics*, *8*(7), 15129-15147.

[12] Bohner, M., Hristova, S., Malinowska, A.B., Morgado, M.L., & Almeida, R. (2022). A generalized proportional Caputo fractional model of multi-agent linear dynamic systems via impulsive control protocol. *Communications in Nonlinear Science and Numerical Simulation*, *115*, 106756.

[13] Boucenna, D., Baleanu, D., Ben Makhlouf, A., & Nagy, A.M. (2021). Analysis and numerical solution of the generalized proportional fractional Cauchy problem. *Applied Numerical Mathematics*, *167*, 173-186.

[14] Ahmad, M., Zada, A., Ghaderi, M., George, R., & Rezapour, S. (2022). On the existence and stability of a neutral stochastic fractional differential system. *Fractal Fractional*, *6*, 203.

[15] Akgül, A., & Baleanu, D. (2021). Analysis and applications of the proportional Caputo derivative. *Advances in Difference Equations*, *2021*, 136.

[16] Jarad, F., Abdeljawad, T., & Alzabut, J. (2017). Generalized fractional derivatives generated by a class of local proportional derivatives. *The European Physical Journal Special Topics*, *226*, 3457-3471.

[17] Naifar, O., Nagy, A.M., Ben Makhlouf, A., Kharrat, M., & Hammami, M.A. (2019). Finite-time stability of linear fractional-order time-delay systems. *International Journal of Robust and Nonlinear Control*, *29*(1), 180-187.

[18] Rezapour, S., Deressa, C.T., & Etemad, S. (2021). On a memristor-based hyperchaotic circuit in the context of nonlocal and nonsingular kernel fractional operator. *Journal of Mathematics*, *2021*, 6027246, 1-21.

[19] Batiha, I.M., Albadarneh, R.B., Momani, S., & Jebril, I.H. (2020). Dynamics analysis of fractional-order Hopfield neural networks. *International Journal of Biomathematics*, *13*(8), 2050083.

[20] Huang, C., Wang, H., & Cao, J. (2023). Fractional order-induced bifurcations in a delayed neural network with three neurons. *Chaos*, *33*, 033143.

[21] Liu, D., Zhu, S., & Chang, W. (2017). Mean square exponential input-to-state stability of stochastic memristive complex-valued neural networks with time varying delay. *International Journal of Systems Science*, *48*(9), 1966-1977.

[22] Li, T., Song, A.G., Fei, S.M., & Guo, Y.Q. (2009). Synchronization control of chaotic neural networks with time-varying and distributed delays. *Nonlinear Analysis Theory, Methods Applications*, *71*, 2372-2384.

[23] Zhang, X., & Yang, C. (2020). Neural network synchronization of fractional-order chaotic systems subject to backlash nonlinearity. *AIP Advances*, *10*(6), 065110.

[24] Wang, R., Zhang, Y., Chen, Y., Chen, X., & Xi, L. (2020). Fuzzy neural network-based chaos synchronization for a class of fractional-order chaotic systems: an adaptive sliding mode control approach. *Nonlinear Dynamics*, *100*, 1275-1287.

[25] Erdelyi, A. (1953). *Higher Transcendental Functions*. Vol. III, New-York: McGraw-Hill.

[26] Ye, H., Gao, J., & Ding, Y. (2007). A generalized Gronwall inequality and its application to a fractional differential equation. *Journal of Mathematical Analysis and Applications*, *328*(2), 1075-1081.